chemosensors

MDPI

Article

Effect of Applied Electrical Stimuli to Interdigitated Electrode Sensors While Detecting 17α-Ethinylestradiol in Water Samples

Paulo M. Zagalo [1,2,*], Paulo A. Ribeiro [2] and Maria Raposo [2,*]

[1] CEFITEC, Departamento de Física, Faculdade de Ciências e Tecnologia, Universidade Nova de Lisboa, 2829-516 Caparica, Portugal
[2] Laboratory of Instrumentation, Biomedical Engineering and Radiation Physics (LIBPhys-UNL), Department of Physics, NOVA School of Science and Technology, Universidade NOVA de Lisboa, 2829-516 Caparica, Portugal; pfr@fct.unl.pt
* Correspondence: p.zagalo@campus.fct.unl.pt (P.M.Z.); mfr@fct.unl.pt (M.R.)

Abstract: The effect of impedance measurements of applied voltage on the detection of 17α-ethiny lestradiol (EE2) in water samples using interdigitated electrodes (IDE) coated or not with thin films, is described. Firstly, the effect of immersion in EE2 aqueous solutions of layer-by-layer films prepared with poly(allylamine hydrochloride) (PAH), graphene oxide (GO), poly(1-(4-(3-carboxy-4-hydroxyphenylazo) benzene sulfonamido) 1,2 ethanediyl, sodium salt) (PAZO), polyethylenimine (PEI) and poly(sodium 4-styrenesulfonate) (PSS) was analyzed. These results demonstrated that PAH/GO films desorb during the immersion on EE2 solutions, while EE2 adsorbs on PAH/PAZO and PEI/PSS films with characteristic time values of 16.7 and 7.1 min, respectively, demonstrating that both films are adequate for the development of EE2 sensors. However, as the adsorption characteristic time is shorter, and the EE2 adsorbed amount is smaller, the PEI/PSS films are more suitable for the development of sensors. The effect of the applied voltage was analyzed using both IDEs covered with PEI/PSS films as well as those uncoated. The capacitance spectra are best fitted to analyze this effect, and the loss tangent spectra are advantageous to analyze the aqueous media. Furthermore, it was concluded that lower voltage values are best suited to perform measurements of this nature, given that higher voltages lead to less reliable results and cause irreparable damage to the sensors.

Keywords: impedance; EE2; interdigitated electrodes; sensors; layer-by-layer; thin films; applied voltage

Citation: Zagalo, P.M.; Ribeiro, P.A.; Raposo, M. Effect of Applied Electrical Stimuli to Interdigitated Electrode Sensors While Detecting 17α-Ethinylestradiol in Water Samples. *Chemosensors* **2022**, *10*, 114. https://doi.org/10.3390/chemosensors10030114

Academic Editors: Paolo Ugo and Nicole Jaffrezic-Renault

Received: 30 January 2022
Accepted: 14 March 2022
Published: 16 March 2022

1. Introduction

Personal care and pharmaceutical products (PPCP) and endocrine-disrupting chemicals (EDC) are an ever-looming concern and have started to become an environmental threat that should no longer be ignored or cast aside [1–4]. Such compounds can be found in a myriad of areas and industries, ranging from medicine (in a multitude of drugs) to hygiene (toothpaste, shampoos), and beauty and skincare (lotions, scrubs, perfumes, makeup), mainly due to revolutionary breakthroughs or advantages made possible by these compounds, such as regulating certain physiological processes, antimicrobial and/or bacteriostatic properties [5,6]. Amongst these chemicals and products are triclosan (5-chloro-2-(2,4-dichlorophenoxy) phenol) (TCS), polychlorinated biphenyls (PCB), chloridane, polyvinyl chloride (PVC), dichlorodiphenyltrichloroethane (DDT), amoxicillin, metaflumizone, methiocarb, estrone (E1), 17β-estradiol (E2) and 17α-ethinylestradiol (EE2), to name a few [7–10]. Although some of these chemicals have already been banned in certain countries, others remain in use, albeit being part of international watchlists, whose main goal is to develop and analyze a great volume of studies regarding their impact on the environment, and posteriorly, allowing for a more informed and educated decision as to their future, be it them being banned, having their use limited and regulated, or allowing their use freely [7–14]. The threat that PPCP and EDC pose against the environment has a nexus to the impossible; due to current technological limitations, to completely remove

these compounds from water that undergoes cleaning processes in wastewater treatment plants (WWTT), results in trace amounts of such products being released into the environment and thus finding their ways into natural water bodies, such as lakes, rivers, seas, and underground waters, among others [15–17]. Even though only diminished concentrations of these chemicals exist in WWTTs, their continued and exponentially growing build-up—as a direct result of our day-to-day usage—have, as demonstrated recently by more and more studies, potential and actual malign consequences for animal and plant life, including humans [18–20]. One of these abovementioned EDCs, EE2, is a synthetic hormonal molecule that is one of the main components of the oral birth control pill ingested by women throughout the world [21]. As stated before, this hormone ends up in natural bodies of water where several studies have shown cases of changes in reproductive organs, mating habits, and even in some extreme situations, mass sterilizations, be it in fauna or flora [22–24]. In humans, there have also been reported studies that connect the presence of EE2 in the environment to a propensity to developing cancer [25,26].

By developing sensor devices, or even an array of sensors based on the electronic tongue (ET) concept [27–29], the issues regarding the detection and monitoring or emergent contaminants, such as PPCP and EDC, can be tackled to transition from a quasi-passive state to a more active and dynamic one, thus providing a valuable set of tools to battle this alarmingly rising health hazard. To this end, one viable option is the use of interdigitated electrodes (IDE) in tandem with systems of electrical measuring devices, as is the case of impedance spectroscopy, to allow the analysis, study, and observation of a diverse pool of samples of varied origins [30]. IDEs are a highly versatile tool for this type of work due to their innate adaptability, be it regarding their configuration, size, geometry, or even their low cost and rather simple manufacturing methods. These advantages have propelled them to reach new heights, namely in their widespread use by the scientific community in the sensor science field [31–33]. In a study developed by Taylor and MacDonald [34], a model was proposed to illustrate the AC electrical behavior of metal electrodes upon their immersion in electrolyte aqueous solutions, and allow its user to observe and analyze the thin film growth on electrode substrates. Additionally, it is also possible to measure spectra of loss tangents as well as capacitance, to infer and attain relevant data related to the sample's capacitive and conductive properties throughout a range of moderate frequencies as well as to demonstrate that the electrical behavior displayed by the electrodes differs based on the frequency zone (high frequencies or low frequencies). This work laid down the path for a multitude of studies on interdigitated electrodes and their potential applications.

One of these studies investigated the variations of the width of the electrodes' digits as well as the distance between them to ascertain how these morphological changes would affect the signal-to-noise ratio and IDE general electrical response [35]. Similarly, there have also been studies that explored the importance of the different geometrical parameters of IDE digits, such as width (W), gap (G), length (L), and height (H). After numerous simulations and attempts, the optimized final version of these electrodes possessed 39 fingers digits and their inherent parameters were as follows: W/G = 1500/500 nm; L = 180 µm; H = 200 nm. Through further simulations and experimental work, several interesting conclusions were drawn: by increasing the contact areas delimited through the height and length of the IDE digits, a larger number of biomolecular interactions could take place, thus increasing the richness of the signal and the information obtained; the width parameter was found to possess a diminished weight as compared to previous studies; and finally, the gap (spacing) between the IDE fingers was reported to be the primary and deciding feature regarding the variation of the sensors' overall sensitivity [36]. Another study reported to have conducted multiple simulations intending to model an impedance-based IDE biosensor, and through this work, it was shown that the dimensions of the IDE configurations (primarily digits' width and gap) would inevitably influence the electric field's magnitude measured. They went on to conclude that electrodes of significantly small dimensions that rely mainly on highly expensive manufacturing techniques generally do not display better

results than similar devices, whose dimensions were faintly bigger and were pointedly less expensive to produce [37].

The aim of this work rested on confirming the results of previous work [38] and achieving optimization of said work for future impedance measurements of thin film-based IDE sensors focused on the detection and monitoring of emergent contaminants (EE2 in this case) in water matrices, to which end, two separate studies were planned and put into practice. Firstly, a study was conducted by spectrophotometry, and was centered around the stability of different combinations of thin films ($(PAH/GO)_5$, $(PAH/PAZO)_5$ and $(PEI/PSS)_5$) to select the one(s) with the best response(s) for this and future related works. Secondly, a study was designed to see in what ways different values of AC voltages applied to the sensors during the aforementioned measurements would influence the quality of both the data received and of each sensor. The information and results attained through the present work will then be implemented in a variety of sensor science experiments with the ultimate goal of obtaining an array of different sensors capable of detecting emergent pollutants (electronic tongue).

2. Materials and Methods

For spectrophotometric measurements, quartz solid supports were used while for the impedance-related measurements, ceramic substrates with gold IDE (200 µm/200 µm) deposited onto their surfaces were used as the base sensor devices, as shown in Figure 1. These ceramic IDE substrates were acquired from DropSens (Asturias, Spain).

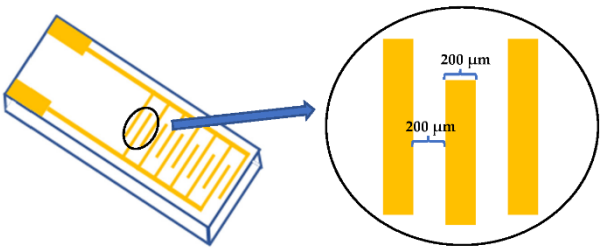

Figure 1. Schematic representation of the ceramic substrates with gold IDE (200 µm/200 µm) acquired from DropSens (Asturias, Spain) and used in this work.

Three different kinds of films are composed of poly(allylamine hydrochloride) (PAH) and graphene oxide (GO) (designated as PAH/GO); PAH and poly(1-(4-(3-carboxy-4-hydroxyphenylazo) benzene sulfonamido) 1,2 ethanediyl, sodium salt) (PAZO) (designated as PAH/PAZO); and polyethylenimine (PEI) and poly(sodium 4-styrenesulfonate) (PSS) (designated as PEI/PSS) were prepared onto both quartz supports and ceramic substrates with gold IDE using the layer-by-layer (LbL) technique. This technique consists of adsorbing alternating layers of polyelectrolyte molecules with opposing electrical charges at a solid/liquid interface onto [39]. One should denote the polyelectrolytes as PAH and PEI are positively charged, while GO, PAZO, and PSS are negatively charged. The adsorption period of each polyelectrolyte layer was of one minute and the concentration of GO aqueous solutions was 10^{-4} M and the monomeric concentration of other polyelectrolyte aqueous solutions was 10^{-2} M. After the adsorption of each polyelectrolyte layer, the solid supports were immediately rinsed with ultrapure water and dried with a nitrogen flux. The prepared thin films contained 5 bilayers adsorbed onto the solid substrates, and henceforth will be referred to as $(PAH/GO)_5$, $(PAH/PAZO)_5$, and $(PEI/PSS)_5$.

As stated above, one intends to develop EE2 sensors, and it is necessary to analyze if EE2 adsorbs on the thin films or if the LbL film deposited on the solid desorbs when immersed in the EE2 aqueous solutions. Therefore, the immersion of the three types of thin films deposited onto quartz substrates in a solution of ultrapure water (pH = 6.5 ± 0.3) spiked with a concentration of 10^{-12} M of 17α-ethinylestradiol were analyzed by measuring the ultraviolet-visible (UV-Vis, Shimadzu, Kyoto, Japan) spectra before and after the thin films were to be immersed for a period of time. The UV-Vis spectra were measured at each

timestamp of 5 min of immersion of the thin films in the EE2 aqueous solution. UV-Vis spectrophotometry was chosen because GO, PAZO, PSS, and EE2 present absorption in the UV-visible region which allows to verify if EE2 molecules adsorb on the LbL films or the molecules of the LbL films desorb on the EE2 solution. The procedure was repeated in increments of 5 min submersions until each thin film reached a time of immersion of 25 min. The UV-Vis spectra were obtained using a double beam spectrophotometer UV-2101PC (Shimadzu, Kyoto, Japan) in transmission mode with a sampling interval between 800 nm and 200 nm, and with a resolution of 0.5 nm. The spectrophotometric measurements were performed by placing both a neat quartz solid support and one with the adsorbed LbL thin film in a double beam system, wherein the source beam is split into two equal beams and each beam penetrates two substrates simultaneously, the remaining one being an uncoated quartz substrate. The photodetectors, located directly after the substrates, are then able to detect the transmittance (fraction of light that traverses the object and exits on the opposite side) of each substrate, which in turn is converted into absorbance. Such a configuration displays the advantage of exclusively allowing the attainment of the absorbance of the deposited thin film. All five polyelectrolytes (PAH, PAZO, GO, PEI, and PSS) and EE2 standards were purchased from Sigma-Aldrich (Darmstadt, Germany).

The ultimate goal of this work rested on the study of the sensors' behavior to varying values of applied voltage while conducting measurements to detect 17α-ethinylestradiol (EE2) in two different waters with different matrix complexities. The water samples used were a commercial Portuguese mineral water (Águas de Luso, Luso, Portugal) (pH = 5.7 $\pm$ 0.3) and tap water (pH = 6.8 $\pm$ 0.1). Throughout this paper, they will be referred to as MW and TW, respectively. These matrices were chosen as the objects of study due to their different complexity levels, and particularly, to investigate how this difference would influence the electrical measurements conducted regarding the detection of EE2. For each water matrix, two types of sensors were prepared: IDE with no film (uncoated), and $(PEI/PSS)_5$ thin films adsorbed on IDE. The thin film deposition was achieved using LbL, following a procedure identical to the one detailed above.

Solutions containing 10^{-12} M of EE2 were prepared for each water, MW, and TW, and both uncoated and thin film sensors were then immersed in these solutions. Several AC voltages applied to the IDE sensors were chosen, and measurements for each voltage were performed: from 25 to 1000 mV. These electrical measurements were conducted using a Solartron 1260 impedance analyzer, Solartron Metrology Limited, Leicester, England, with a frequency range of (1–1 M) Hz, and all measurements were repeated in triplicate to guarantee that the data was reliable and reproducible.

With all the data collected from the impedance analyzer, the electrical features, and properties associated with the conducted measurements underwent a statistical treatment via the principal component analysis (PCA) method, thus allowing for the volume of data to be compacted while not losing any vital information, and to analyze the correlation between all the voltage values and the sensors' detection capabilities in a separate dimension specific to orthogonal components [40]. The core concept behind an electronic tongue rests on the use of a vast collection of sensing devices and then correlating the resulting data obtained with an equally grand quantity of samples. This goes perfectly together with the basis of PCA, where to achieve better results one must make use of a considerable number of samples, each with a vast number of variables [41]; however, there are also studies showing that smaller quantities of samples yield equally valid and good quality results [42]. For the PCA analysis, we used data consisting of impedance, capacitance, real and imaginary components of impedance, and loss tangent, which, as mentioned above, were obtained for a range of frequencies between 1 Hz and 1 MHz. This statistical treatment was applied to every IDE sensor and both waters used.

3. Results

3.1. Studies of Stability of Thin Films

To analyze the stability of the prepared thin films when immersed in aqueous solutions, the $(PAH/GO)_5$, $(PAH/PAZO)_5$, and $(PEI/PSS)_5$ thin films deposited onto the surface of quartz substrates were immersed in solutions of EE2 with a concentration of 10^{-12} M during increments of 5 min and up to a total of 25 min of immersion. After every set of 5 min, the UV-Vis spectra of the films were measured. Figure 2a–c shows the evolution of the absorbance at a wavelength of 280 nm with the time of immersion of the $(PAH/GO)_5$, $(PAH/PAZO)_5$, $(PEI/PSS)_5$ thin films, respectively, in the EE2 solutions. Through the achieved data, it is possible to observe that the absorbance of each film was influenced by the immersion times.

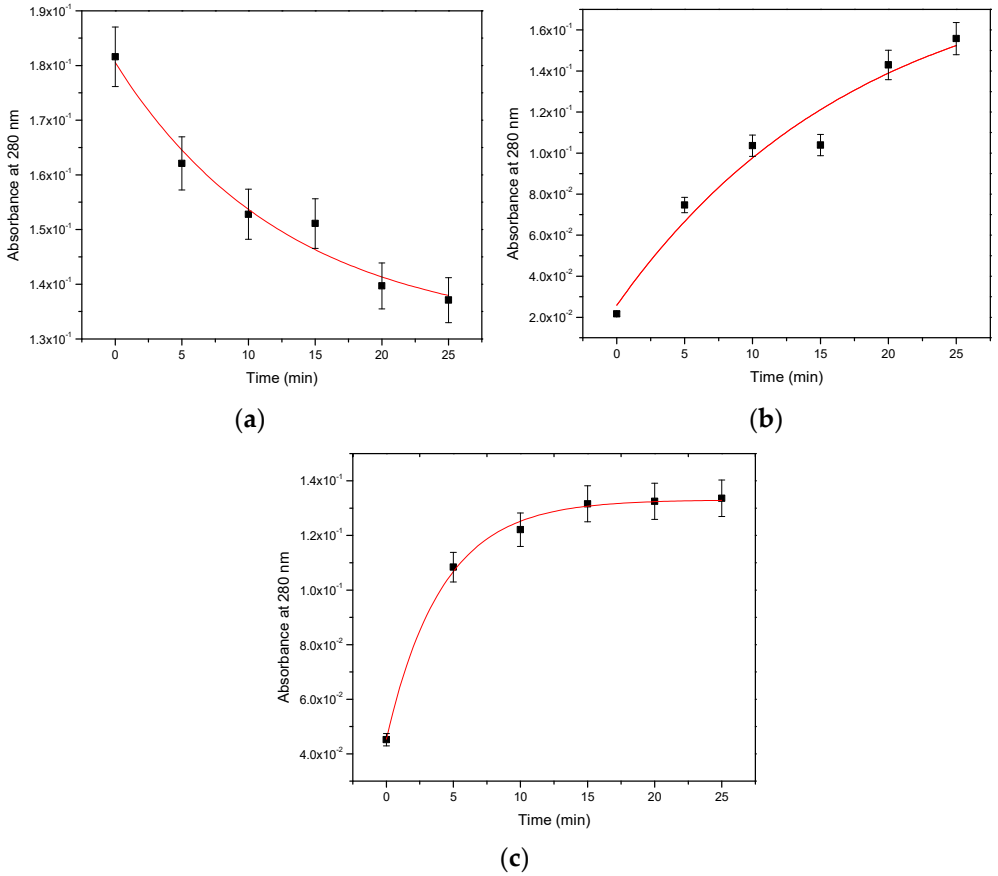

Figure 2. Absorbance at 280 nm of films over time submerged in a solution of ultrapure water spiked with a concentration of EE2 of 10^{-12} M of (**a**) $(PAH/GO)_5$, (**b**) $(PAH/PAZO)_5$, (**c**) $(PEI/PSS)_5$ thin films.

Two tendencies are observed from the graphs in Figure 2. In Figure 2a, the absorbance decreases exponentially with the immersion time, indicating that the GO molecules of the $(PAH/GO)_5$ film are being desorbed when immersed in the EE2 solution. This result demonstrates that these films are not adequate to be used as sensors of EE2 molecules, as the calculated characteristic time of 11.6 min is smaller than the electrical measuring time. The data achieved from spectra of $(PAH/PAZO)_5$ and $(PEI/PSS)_5$, Figure 2b,c, respectively, demonstrate that the absorbance increases exponentially with the immersion, which indicates that the EE2 molecules are being adsorbed on these films. The adsorption characteristic times calculated from these data are 16.7 and 7.1 min for $(PAH/PAZO)_5$ and $(PEI/PSS)_5$ films, respectively. These values indicate that the adsorption of EE2 molecules is faster on $(PEI/PSS)_5$ films while the EE2 adsorbed amount on $(PAH/PAZO)_5$ films is twice the one on $(PEI/PSS)_5$ films, indicating that the EE2 molecules have more

affinity to $(PAH/PAZO)_5$ films. These results indicate that both films are adequate for the development of EE2 sensors. However, as the adsorption characteristic time is shorter and the EE2 adsorbed amount is smaller, the $(PEI/PSS)_5$ films are more adequate for the development of sensors.

3.2. Effect of Applied Voltage on the Interdigitated Sensors Characterization

$(PEI/PSS)_5$ films were subsequently deposited on the surface of gold IDE (200 µm/200 µm) and were used in a series of impedance-related studies. Figures 3 and 4 illustrate, respectively, the capacitance and electric modulus spectra obtained through the electrical measurements of the IDE sensors, uncoated (Figure 3a,c) and with $(PEI/PSS)_5$ film (Figure 3b,d), for varying applied voltages while immersed in solutions of both MW (Figure 3a,b) and TW (Figure 3c,d), with a 10^{-12} M concentration of EE2. It should be referred that the error bar measured values for these spectra were not included, given that both measurements conducted are dependent on the frequency, present values are lower than 1%, and it allows for better clarity and interpretation of the plots present in Figures 3 and 4.

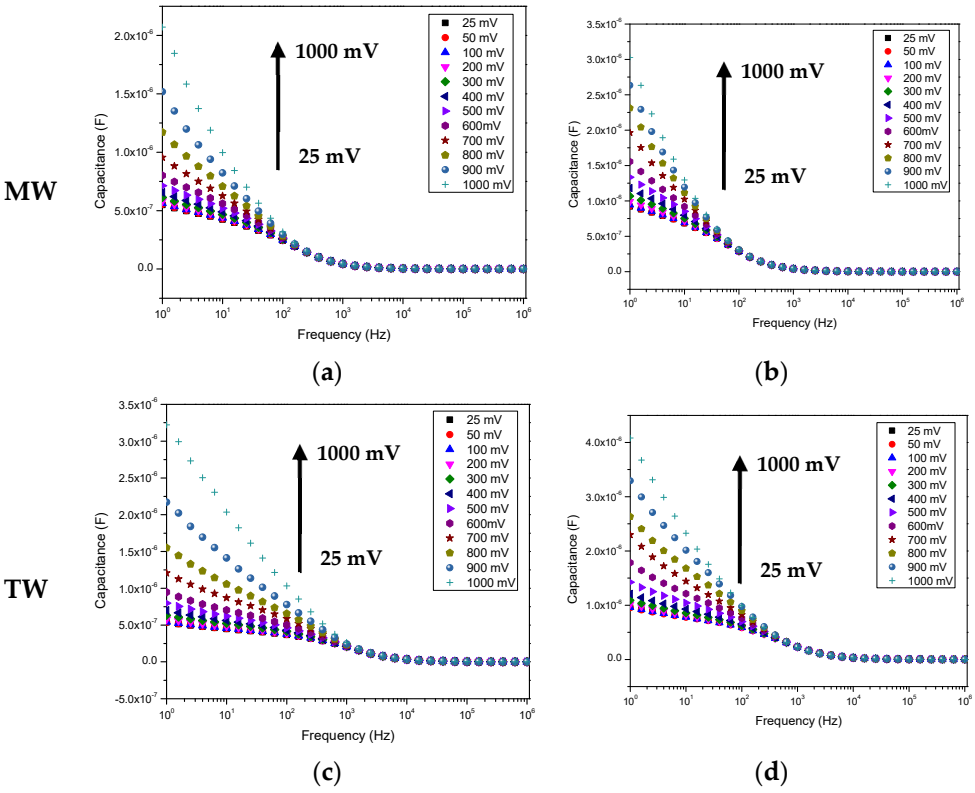

Figure 3. Capacitance spectra of the sensor devices, when immersed in water solutions with a concentration of 10^{-12} M of EE2, for a range of applied voltages: (**a**) uncoated IDE in MW, (**b**) IDE coated with $(PEI/PSS)_5$ film in MW, (**c**) uncoated IDE in TW, (**d**) IDE coated with $(PEI/PSS)_5$ in TW. The relative error is less than 1%. Arrow indicates the evolution of voltage values, from 25 mV up to 1000 mV.

Through the analysis of Figure 3, it is possible to infer that there is a correlation between the capacitance and the varying (and increasing) voltage. In the region of lower frequencies, it becomes clear that not only is it easier to distinguish each voltage, but also that there is an ordered sequence ranging from the lowest (25 mV) to the highest (1000 mV) voltage value. This information indicates that this type of measurement is vital to observe how the gradual increase in applied voltage to the measuring sensor device behaves and impacts the electrical data output. While comparing the waters in which the measurements were performed, one can verify that there is an improvement in capacitance for the sensors

immersed in tap water regarding the ones in mineral water. However, from the plots in Figure 3, one can observe that the higher the voltage used, the higher the capacitance, which suggests that the sensors can be more susceptible to signal fluctuations and thus display lower stability when compared to lower voltages. This issue is further examined in the discussion section. Figure 5a,b shows the correlation of capacitance at 1 Hz and M″ at 2×10^5 Hz, respectively, with the varying values of voltage. Both plots allow us to confirm what can be seen above in Figures 3 and 4, in the sense that capacitance proves to be a far better and more valuable tool at showing how each type of sensor responds to the gradual increase of voltage. While Figure 5a shows an exponential tendency for capacitance to increase with voltage and even allows to see a sort of pairing between the types of sensors (uncoated and coated with $(PEI/PSS)_5$), Figure 5b does not provide useful information in this regard, indicating that M″ is not a good/suitable characterization resource tool in this work.

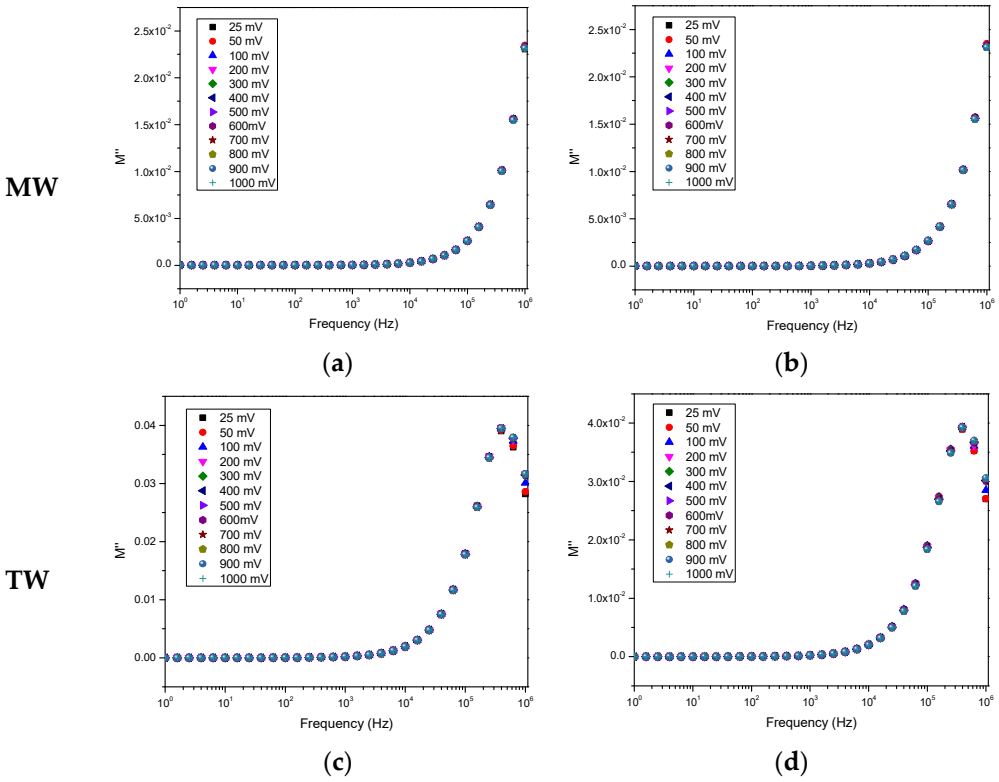

Figure 4. Spectra of the imaginary component of the electrical modulus (M″) of the sensor devices, when immersed in water solutions with a concentration of 10^{-12} M of EE2, for a range of applied voltages: (**a**) uncoated IDE in MW, (**b**) IDE coated with $(PEI/PSS)_5$ film in MW, (**c**) uncoated IDE in TW, (**d**) IDE coated with $(PEI/PSS)_5$ in TW. The relative error is less than 1%.

Having seen how each sensor independently reacted to the voltage variation, a need arose to investigate how similar sensors behaved in different waters, which is depicted below in Figure 6.

Figure 6a,b illustrated how similar sets of sensors (uncoated and coated with $(PEI/PSS)_5$, respectively) react when in the presence of different waters. Both plots convey similar information, given that in both, the loss tangent allows to differentiate between water types, MW and TW, through a right shift of the tap water-related curves, and also displays the ability to better distinguish each voltage applied (TW being the best scenario) while simultaneously exhibiting an ordered sequence of these values, as indicated by the red and blue arrows in Figure 6.

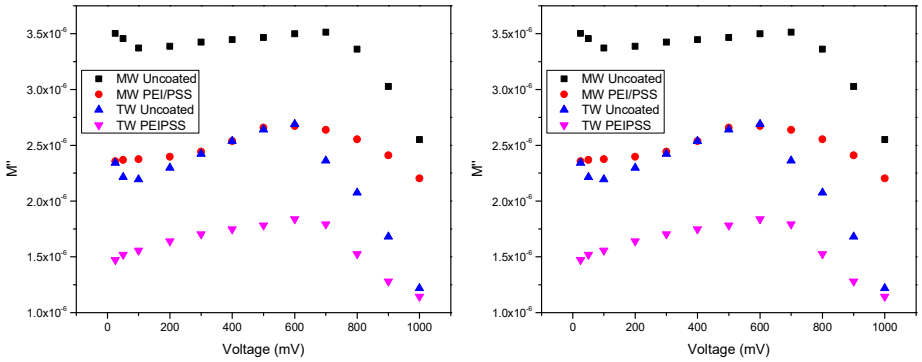

Figure 5. Plots of the (**a**) capacitance and (**b**) imaginary component of the electrical modulus (M″) as functions of the varying voltage applied to the sensors (uncoated and with a $(PEI/PSS)_5$ thin film) in both types of water, MW and TW, for 1 Hz and 2×10^5 Hz, respectively. The relative error is less than 1%.

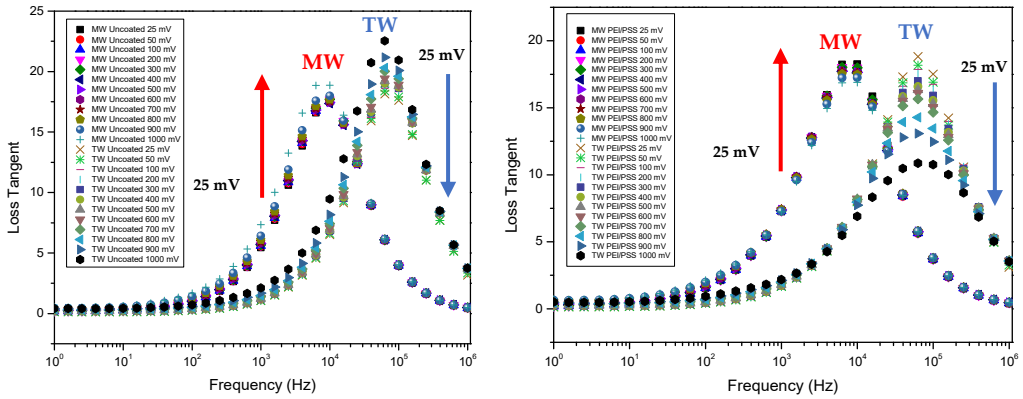

Figure 6. Loss tangent spectra for (**a**) uncoated sensors and (**b**) coated with a $(PEI/PSS)_5$ film, for both mineral and tap water. Red and blue arrows indicate the evolution of the voltage values, from 25 mV up to 1000 mV. The relative error is less than 1%.

Figure 7 shows three sets of images referring to the IDE sensors used in this work, obtained through optical microscopy.

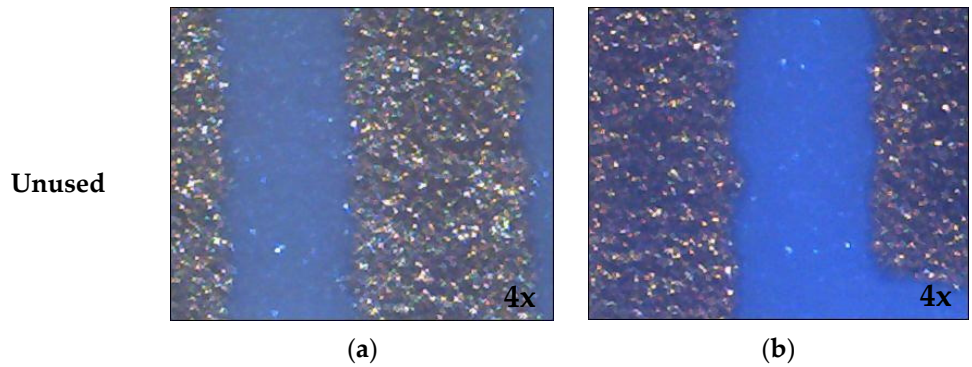

Figure 7. *Cont.*

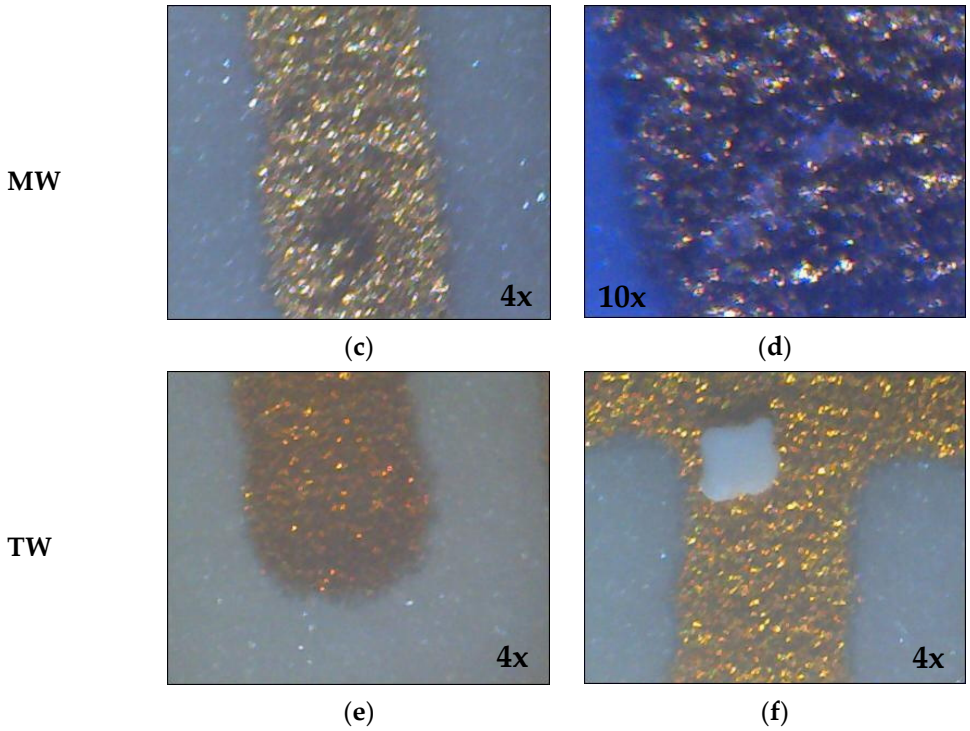

Figure 7. Optical microscopy images of the IDE sensors showing the damage caused by the increasingly higher values of the voltage applied during the impedance measurements. (**a**) Uncoated IDE before applying voltage, (**b**) IDE coated with $(PEI/PSS)_5$ film before applying voltage, (**c**) uncoated IDE after applying voltage while immersed in MW, (**d**) IDE coated with $(PEI/PSS)_5$ film after applying voltage while immersed in MW, (**e**) uncoated IDE after applying voltage while immersed in TW, (**f**) IDE coated with $(PEI/PSS)_5$ film after applying voltage while immersed in TW.

The images captured during the optical microscopy analysis, presented in Figure 7, give an immediate and quite evident visual confirmation of the impact that increasing AC voltages applied to each sensor have during the impedance measurements.

4. Discussion

Figure 8 includes the PCA graphs calculated and plotted to give a more detailed analysis of the phenomenon observed in Figure 3, and also to demonstrate how the data containing all the information regarding each sensor and type of water would translate into a visual representation.

The principal component analysis plots, present in Figure 8, allow for an in-depth analysis of how both types of IDE sensors respond to the different waters used in this study. In Figure 8a, a plot of PC1 as a function of PC2 was plotted with all the electrical data collected during these measurements for both sensors, uncoated and with a $(PEI/PSS)_5$ film, in the two waters, MW and TW. From this graph, it can be perceived that Principal Component 1 is a strong tool when it comes to separating and distinguishing the different voltages used (even displaying a tendency and an ordered sequence), while Principal Component 2 allows for a clear distinction between MW and TW. Both strong and valuable points were then further examined by plotting the graphs depicted in Figure 8b,c.

No damage can be seen or found in both uncoated sensors and the one coated with $(PEI/PSS)_5$ film, Figure 7a,b, respectively, before being submerged in the water solutions and having any voltage applied to the sensors. It is only when we analyze Figure 7c,d, in which the sensors were immersed in mineral water, that it is possible to observe some differences from the antecedent images, due to some burnt regions in the uncoated sensor. On the thin film coated sensor, this evidence is punctuated by larger burnt areas and some spots that show erosion down to the gold IDE, indicating that in those regions, not only

does the $(PEI/PSS)_5$ film get removed but even the gold layer of the electrode suffers a degree of destruction.

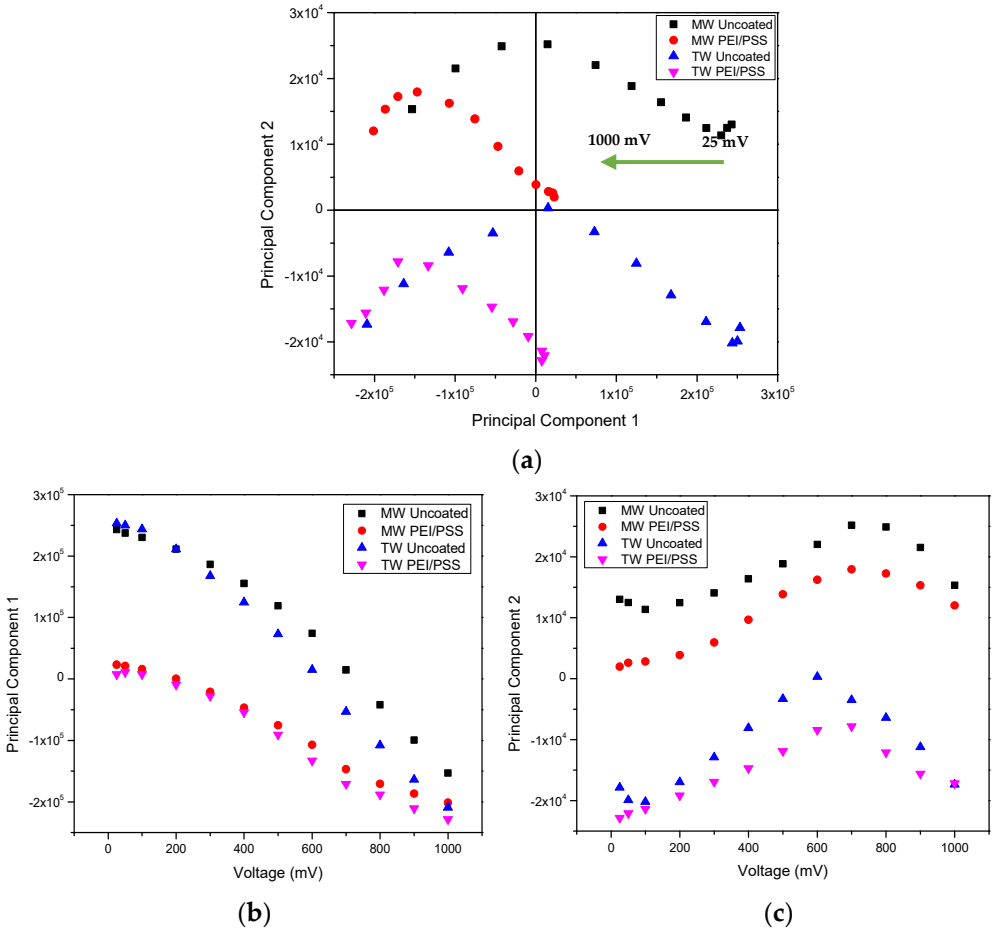

Figure 8. PCA plots of all IDE (uncoated and with $(PEI/PSS)_5$ film) in both types of water used: (**a**) PC1 vs. PC2, (**b**) PC1 vs. voltage applied, (**c**) PC2 vs. voltage applied. The green arrow illustrates the ordered sequence of voltage values, from 25 mV up to 1000 mV.

However, this effect reaches a peak of damage in the images that depict the measurements undergone in tap water (Figure 7e,f). Here (Figure 7e), the uncoated sensor changes coloration, going from shiny gold to rust orange and the extremities of the interdigitated electrodes suffer alteration, losing the characteristic rectangular shape for a more rounded and smoothed shape as a direct result of the high voltage values used. In the image pertaining to the $(PEI/PSS)_5$ sensor (Figure 7f), from a top-to-bottom observation, the thin film has almost in its entirety been removed due to the gold layer presenting a coloration akin to an uncoated sensor and displaying resistance values like a brand-new IDE sensor. Furthermore, large portions of the gold layer have been thoroughly corroded, showing the ceramic substrate below. From this image, it can be concluded that increasing the AC voltage values that are applied to the sensor strongly influence their integrity and that the phenomenon is directly proportional to the complexity of the water matrix, i.e., the higher the matrix's complexity, the greater the damage suffered by the sensors will be. These results agree with the ones reported in [38], presenting a confirmation of the suggested build-up of electrochemical reactions that hindered the sensors' performance at high voltage values that caused reproducibility issues.

5. Conclusions

In this work, we focused on investigating the impact that different values of AC voltage applied to thin films interdigitated electrodes have on their performance as sensing

devices, to which end, the study was divided into two separate parts. In the initial stage, an adsorption/desorption analysis was conducted on three distinct thin film combinations, $(PAH/GO)_5$, $(PAH/PAZO)_5$, and $(PEI/PSS)_5$, while being immersed in solutions of ultra-pure water containing a known concentration of 10^{-12} M of EE2. This was achieved by depositing the abovementioned sets of thin films onto quartz substrates, immersing the films in the EE2 solutions in 5 min intervals (total of 25 min), and measuring the resulting absorbance spectra in a UV-Vis spectrophotometer. Having displayed the best and most stable results, $(PEI/PSS)_5$ thin films were chosen as the sensing layer of the IDE sensors. The second part of this study was then centered around the variation of the voltage values that were being applied to the sensors during measurements of impedance spectroscopy, while immersed in solutions of mineral and tap waters spiked with a 10^{-12} M concentration of EE2. From these measurements, spectra of capacitance, loss tangent, and an imaginary part of the electrical modulus were plotted and subsequently analyzed, to characterize the sensors' behavior when subjected to varying voltages.

The data obtained allowed us to conclude that both the capacitance and loss tangent were the better-fitted tools to observe these variations, which in turn, demonstrated that for lower values of voltage, more reliable, consistent, and reproducible results were achieved. In particular, loss tangent spectra did not allow for observations of a clear distinction between each voltage curve, and additionally, it is sensitive to the type of water used (and is able to differentiate between them). To further infer the sensors' ability to react to each different voltage applied, PCA plots were generated and granted a more in-depth view into this issue, making it clear that, for each voltage, there was a unique and separate reaction from the sensors. By combining both parts of this work, one can conclude that (1) $(PEI/PSS)_5$ thin films exhibit the most stable behavior and should be used in future experiments as a sensing layer for EE2; and (2) when conducting impedance spectroscopy measurements, lower voltage values should be used instead of higher ones due to their innately better and more reliable response.

Author Contributions: Conceptualization, P.M.Z. and M.R.; methodology, P.M.Z.; software, P.M.Z.; validation, P.M.Z.; formal analysis, P.M.Z. and M.R.; literature review, P.M.Z. and M.R.; resources, M.R. and P.A.R.; data curation, P.M.Z. and M.R.; writing—original draft preparation, P.M.Z.; writing—review and editing, P.M.Z. and M.R.; visualization, P.M.Z.; supervision, P.A.R. and M.R.; project administration, P.A.R. and M.R.; funding acquisition, P.A.R. and M.R. All authors have read and agreed to the published version of the manuscript.

Funding: This research was funded by Fundação para a Ciência e a Tecnologia (FCT-MCTES), the Radiation Biology and Biophysics Doctoral Training Programme (RaBBiT, PD/00193/2012), PTDC/FIS-NAN/0909/2014, the CEFITEC Unit (UIDB/00068/2020), UIDB/04559/2020 (LIBPhys) and UIDP/04559/2020 (LIBPhys), and a scholarship, grant number PD/BD/142767/2018, to Paulo M. Zagalo, from the RaBBiT Doctoral Training Programme and the Bilateral Project entitled "Deteção de Estrogénio um Contaminante Emergente-em Corpos Hídricos" within the scope of "Cooperação Transnacional_FCT (Portugal)-CAPES (Brazil) 2018".

Institutional Review Board Statement: Not applicable.

Informed Consent Statement: Not applicable.

Data Availability Statement: Not applicable.

Acknowledgments: Paulo M. Zagalo acknowledges his fellowship PD/BD/142767/2018 from the RABBIT Doctoral Programme.

Conflicts of Interest: The authors declare no conflict of interest. The funders had no role in the design of the study; in the collection, analyses, or interpretation of data; in the writing of the manuscript, or in the decision to publish the results.

References

1. Wang, Y.; Yang, Q.; Dong, J.; Huang, H. Competitive adsorption of PPCP and humic substances by carbon nanotube membranes: Effects of coagulation and PPCP properties. *Sci. Total Environ.* **2018**, *619–620*, 352–359. [CrossRef] [PubMed]
2. Duca, G.; Boldescu, V. Pharmaceuticals and Personal Care Products in the Environment. In *The Role of Ecological Chemistry in Pollution Research and Sustainable Development*; NATO Science for Peace and Security Series C: Environmental Security; Bahadir, A.M., Duca, G., Eds.; Springer: Dordrecht, The Netherland, 2009; pp. 27–35. [CrossRef]
3. Liu, J.L.; Wong, M.H. Pharmaceuticals and personal care products (PPCPs): A review on environmental contamination in China. *Environ. Int.* **2013**, *59*, 208–224. [CrossRef] [PubMed]
4. Meyer, M.F.; Powers, S.M.; Hampton, S.E. An Evidence Synthesis of Pharmaceuticals and Personal Care Products (PPCPs) in the Environment: Imbalances among Compounds, Sewage Treatment Techniques, and Ecosystem Types. *Environ. Sci. Technol.* **2019**, *53*, 12961–12973. [CrossRef] [PubMed]
5. Marques, I.; Magalhães-Mota, G.; Pires, F.; Sério, S.; Ribeiro, P.A.; Raposo, M. Detection of traces of triclosan in water. *Appl. Surf. Sci.* **2017**, *421*, 142–147. [CrossRef]
6. Boxall, A.B.; Rudd, M.A.; Brooks, B.W.; Caldwell, D.J.; Choi, K.; Hickmann, S.; Innes, E.; Ostapyk, K.; Staveley, J.P.; Verslycke, T.; et al. Pharmaceuticals and personal care products in the environment: What are the big questions? *Environ. Health Perspect.* **2012**, *120*, 1221–1229. [CrossRef] [PubMed]
7. Vella, K. Commission Implementing Decision (EU) 2018/840 of 5 June 2018. *Off. J. Eur. Union*. **2018**, 1–4. Available online: https://eur-lex.europa.eu/legal-content/EN/TXT/?uri=CELEX%3A32018D0840 (accessed on 16 December 2021).
8. da Cunha, D.L.; Camargo da Silva, S.M.; Bila, D.M.; da Mota Oliveira, J.L.; de Novaes Sarcinelli, P.; Larentis, A.L. Regulation of the synthetic estrogen 17α-ethinylestradiol in water bodies in Europe, the United States, and Brazil. *Cad. De Saude Publica* **2016**, *32*, 1–12. [CrossRef]
9. UNESCO. Chemical contaminants: Those invisible additives in our drink. *A World Sci.* **2011**, *9*, 18–24.
10. European Commission. Water Framework Directive 2000/60/EC. *Off. J. Eur. Communities* **2000**, *L 269*, 1–15.
11. Hrkal, Z.; Eckhardt, P.; Hrabánková, A.; Novotná, E.; Rozman, D. PPCP monitoring in drinking water supply systems: The example of Káraný waterworks in Central Bohemia. *Water* **2018**, *10*, 1852. [CrossRef]
12. Braig, S.; Delisle, K.; Noël, M. Water Quality Assessment and Proposed Objectives for Burrard Inlet: Pharmaceuticals & Personal Care Products Technical Report. Prepared for Tsleil-Waututh Nation and the Province of B.C.; 2019. Available online: https://www2.gov.bc.ca/assets/gov/environment/air-land-water/water/waterquality/water-quality-objectives/2020-03-31_biwqos_ppcpsdoc.pdf (accessed on 16 December 2021).
13. Priya, A.K.; Gnanasekaran, L.; Rajendran, S.; Qin, J.; Vasseghian, Y. Occurrences and removal of pharmaceutical and personal care products from aquatic systems using advanced treatment—A review. *Environ. Res.* **2022**, *204*, 112298. [CrossRef] [PubMed]
14. Ricky, R.; Shanthakumar, S. Phycoremediation integrated approach for the removal of pharmaceuticals and personal care products from wastewater—A review. *J. Environ. Manag.* **2022**, *302*, 113998. [CrossRef] [PubMed]
15. Buchberger, W. Current approaches to trace analysis of pharmaceuticals and personal care products in the environment. *J. Chromatogr. A* **2011**, *1218*, 603–618. [CrossRef] [PubMed]
16. Yang, Y.Y.; Zhao, J.L.; Liu, Y.S.; Liu, W.R.; Zhang, Q.Q.; Yao, L.; Hu, L.X.; Zhang, J.N.; Jiang, Y.X.; Ying, G.G. Pharmaceuticals and personal care products (PPCPs) and artificial sweeteners (ASs) in surface and ground waters and their application as indication of wastewater contamination. *Sci. Total Environ.* **2018**, *616–617*, 816–823. [CrossRef] [PubMed]
17. Ebele, A.J.; Abou-Elwafa Abdallah, M.; Harrad, S. Pharmaceuticals and personal care products (PPCPs) in the freshwater aquatic environment. *Emerg. Contam.* **2017**, *3*, 1–16. [CrossRef]
18. Raccanelli, S.; Libralato, S.; Tundo, P. *Fate of Persistent Organic Pollutants in the Venice Lagoon: From the Environment to Human Beings through Biological Exploitation?* Springer Science + Business Media B.V.: Berlin/Heidelberg, Germany, 2009; pp. 15–25. [CrossRef]
19. Sengar, A.; Vijayanandan, A. Human health and ecological risk assessment of 98 pharmaceuticals and personal care products (PPCPs) detected in Indian surface and wastewaters. *Sci. Total Environ.* **2022**, *807*, 150677. [CrossRef] [PubMed]
20. Adeleye, A.S.; Xue, J.; Zhao, Y.; Taylor, A.A.; Zenobio, J.E.; Sun, Y.; Han, Z.; Salawu, O.A.; Zhu, Y. Abundance, fate, and effects of pharmaceuticals and personal care products in aquatic environments. *J. Hazard. Mater.* **2022**, *424*, 127284. [CrossRef] [PubMed]
21. Yu, Z.; Xiao, B.; Huang, W.; Peng, P. Sorption of steroid estrogens to soils and sediments. *Environ. Toxicol. Chem.* **2004**, *23*, 531–539. [CrossRef] [PubMed]
22. Clubbs, R.L.; Brooks, B.W. Daphnia magna responses to a vertebrate estrogen receptor agonist and an antagonist: A multigenerational study. *Ecotoxicol. Environ. Saf.* **2007**, *67*, 385–398. [CrossRef]
23. Essandoh, H.M.K.; Tizaoui, C.; Mohamed, M.H.A. Removal of Estrone (E1), 17β-Estradiol (E2) and 17α-Ethinylestradiol (EE2) During Soil Aquifer Treatment of a Model Wastewater. *Sep. Sci. Technol.* **2012**, *47*, 777–787. [CrossRef]
24. Ankley, G.T.; Feifarek, D.; Blackwell, B.; Cavallin, J.E.; Jensen, K.M.; Kahl, M.D.; Poole, S.; Randolph, E.; Saari, T.; Villeneuve, D.L. Re-evaluating the Significance of Estrone as an Environmental Estrogen. *Environ. Sci. Technol.* **2017**, *51*, 4705–4713. [CrossRef] [PubMed]
25. Adeel, M.; Song, X.; Wang, Y.; Francis, D.; Yang, Y. Environmental impact of estrogens on human, animal and plant life: A critical review. *Environ. Int.* **2017**, *99*, 107–119. [CrossRef] [PubMed]
26. Shore, L.S.; Shemesh, M. Estrogen as an Environmental Pollutant. *Bull. Environ. Contam. Toxicol.* **2016**, *97*, 447–448. [CrossRef] [PubMed]

27. Magro, C.; Mateus, E.P.; Raposo, M.; Ribeiro, A.B. Overview of electronic tongue sensing in environmental aqueous matrices: Potential for monitoring emerging organic contaminants. *Environ. Rev.* **2018**, *27*, 1–13. [CrossRef]
28. Yousefi-Nejad, S.; Heidarbeigi, K.; Roushani, M. Electronic tongue as innovative instrument for detection of crocin concentration in saffron (Crocus sativus L.). *J. Food Sci. Technol.* **2022**. [CrossRef]
29. Elamine, Y.; Inácio, P.M.C.; Lyoussi, B.; Anjos, O.; Estevinho, L.M.; da Graça Miguel, M.; Gomes, H.L. Insight into the sensing mechanism of an impedance based electronic tongue for honey botanic origin discrimination. *Sens. Actuators B Chem.* **2019**, *285*, 24–33. [CrossRef]
30. Ibrahim, M.; Claudel, J.; Kourtiche, D.; Nadi, M. Geometric parameters optimization of planar interdigitated electrodes for bioimpedance spectroscopy. *J. Electr. Bioimpedance* **2013**, *4*, 13–22. [CrossRef]
31. Mukhopadhyay, S.C. Sensing and Instrumentation for a Low Cost Intelligent Sensing System. In Proceedings of the SICE-ICASE International Joint Conference, Bexco, Busan, Korea, 18–21 October 2016; pp. 1075–1080. [CrossRef]
32. Mukhopadhyay, S.C.; Gooneratne, C.P.; Demidenko, S.; Sen Gupta, G. Low cost sensing system for dairy products quality monitoring. In Proceedings of the 2005 International Instrumentation and Measurement Technology Conference, Ottawa, ON, Canada, 17–19 May 2005; pp. 244–249, ISBN 0-7803-8880-1.
33. Van Gerwen, P.; Laureys, W.; Huyberechts, G.; Op De Beeck, M.; Baert, K.; Suls, J.; Varlan, A.; Sansen, W.; Hermans, L.; Mertens, R. Nanoscaled interdigitated electrode arrays for biochemical sensors. *Int. Conf. Solid-State Sens. Actuators Proc.* **1997**, *2*, 907–910. [CrossRef]
34. Taylor, D.M.; Macdonald, A.G. AC admittance of the metal/insulator/electrolyte interface. *J. Phys. D Appl. Phys.* **1987**, *20*, 1277–1283. [CrossRef]
35. Döring, J.; Tharmakularajah, L.; Krieger, K. Study of Interdigital Electrode Structures for the Detection of Water Spray, GMA/ITG-Fachtagung Sensoren und Messsysteme, P2: Messsysteme. Available online: https://www.ama-science.org/proceedings/details/3476 (accessed on 16 December 2021).
36. Singh, K.V.; Whited, A.M.; Ragineni, Y.; Barrett, T.W.; King, J.; Solanki, R. 3D nanogap interdigitated electrode array biosensors. *Anal. Bioanal. Chem.* **2010**, *397*, 1493–1502. [CrossRef]
37. MacKay, S.; Hermansen, P.; Wishart, D.; Chen, J. Simulations of interdigitated electrode interactions with gold nanoparticles for impedance-based biosensing applications. *Sensors* **2015**, *15*, 22192. [CrossRef] [PubMed]
38. Zagalo, P.M.; Magro, C.; Ribeiro, P.A.; Raposo, M. Applied Voltage Effect in Lbl Sensors While Detecting 17α-Ethinylestradiol in Water Samples. *Chem. Proc.* **2021**, *5*, 460. [CrossRef]
39. Decher, G.; Schmitt, J. Fine-Tuning of the film thickness of ultrathin multilayer films composed of consecutively alternating layers of anionic and cationic polyelectrolytes. *Prog. Colloid Polym. Sci.* **2007**, *89*, 160–164.
40. Jackson, J.; Edward, A. *Users Guide to Principal Components*; John Wiley & Sons: Hoboken, NJ, USA, 2003; ISBN 0-471-47134-8.
41. Osborne, J.W.; Costello, A.B. Sample size and subject to item ratio in principal components analysis. *J. Biom. Biostat.* **2010**, *9*, 11. [CrossRef]
42. Giacometti, J.A.; Shimizu, F.M.; Carr, O.; Oliveira, O.N. A Guiding Method to Select and Reduce the Number of Sensing Units in Electronic Tongues. In Proceedings of the 2016 IEEE Sensors, Orlando, FL, USA, 30 October–3 November 2016; pp. 1–3.